Jackson, S. D.; Sabella, A.; Hemming, Alexander Vaughan; Bennetts, Shayne; Lancaster, David George.
High-power 83 W holmium-doped silica fiber laser operating with high beam quality, *Optics Letters*, 2007; 32(3):241-243.

High-power 83 W holmium-doped silica fiber laser operating with high beam quality

Stuart D. Jackson

Optical Fibre Technology Centre, The University of Sydney, 206 National Innovation Centre,
Australian Technology Park, 1430 Eveleigh, Sydney, Australia

Alex Sabella, Alex Hemming, Shayne Bennetts, and David G. Lancaster

Defence Science and Technology Organisation, P.O. Box 1500, Edinburgh, South Australia, Australia

Received August 31, 2006; revised October 19, 2006; accepted October 31, 2006;
posted November 2, 2006 (Doc. ID 74640); published January 12, 2007

A high-power 83 W cladding-pumped Tm^{3+}-Ho^{3+}-doped silica fiber laser is reported. Using bidirectional 793 nm diode pumping, a maximum slope efficiency of 42% was produced after a threshold launched pump power of 12 W was exceeded. The laser operated at wavelengths near 2105 nm with moderate beam quality, i.e., $M^2 \sim 1.5$. Further power scaling of the fiber laser was limited by thermal failure of the fiber ends.

OCIS codes: 140.3510, 140.3480.

The well-known high beam quality and high efficiency properties of fiber-based lasers and amplifiers have made these systems subject to a significant degree of interest. Kilowatt output power,[1] narrowband emission,[2] and high-power mode-locked operation[3] are now readily available from these sources in the $1-1.5\ \mu m$ region of the near-infrared spectrum. Widening the wavelength range further into the infrared, however, remains a significant challenge. The recent progress[4] in Tm^{3+}-doped silica $2\ \mu m$ fiber laser research has established that the high-power and high efficiency characteristics of fiber lasers can also be extended to the generation of mid-infrared radiation.

For a range of applications including nonlinear optics, medicine, and sensing, a simple, efficient, and robust source of high-power $2.1\ \mu m$ radiation is desirable. The ${}^5I_7 \rightarrow {}^5I_8$ transition in Ho^{3+}-doped silica is clearly the most obvious choice, however; since the first demonstrations of the singly Ho^{3+}-doped silica[5] and the Tm^{3+}-Ho^{3+}-doped silica[6] fiber lasers, little progress has been made to augment the output power to the levels commensurate with lamp-pumped[7–9] ($\sim$62 W) and diode-pumped[10] ($\sim$20 W) Ho^{3+}-based solid-state lasers. Indeed, these bulk laser demonstrations have involved either cryogenically cooled Ho:YLF and Ho:YAG or complex in-band pumping schemes using diode-pumped Tm:YLF lasers to achieve low thermal loading and a high storage efficiency.

In this Letter, we present the results of a directly diode-pumped Tm^{3+}-Ho^{3+}-doped silica fiber laser in which the output power has been augmented to 83 W, while producing a good quality output beam with reasonably low noise characteristics. With the use of low-concentration Tm^{3+}, sensitized Ho^{3+}-doped double-clad optical fiber, slope efficiencies just exceeding the Stokes efficiency limit have been produced.

The fibers used for the experiments were fabricated in house using the well-established techniques of modified chemical vapor deposition and solution doping. The $Tm^{3+}:Ho^{3+}$ concentration ratio in the solution used to dope the frit of the preform was set at a value of 10:1, a ratio that was taken from the literature relating to Tm^{3+}-Ho^{3+}-doped crystals. The core diameter was $20\ \mu m$, and for a fiber bend radius of 50 mm, the NA was estimated to be 0.08 (by imaging the laser output in the near field using a Spiricon Pyrocam); hence the core was close to supporting only a single transverse mode. The pump core cross section was shaped into a hexagon (D-shaped) and was surrounded by a low-index UV-curable fluoropolymer to create a NA of $\sim$0.4 for the pump light. The absorption coefficient of the fiber was measured to be $4.2\ dBm^{-1}$ for a pump wavelength centered at 793 nm.

Figure 1 displays the experimental setup used to pump both ends of the fiber. The large difference between the pump and laser wavelength necessitates the use of separate lenses to independently focus the pump and collimate the output from the fiber laser. For collimating the laser output a $f = 12$ mm antireflection (AR)-coated plano–convex ZnSe lens was used. A dichroic mirror was butted to one end of the fiber to provide high reflectivity at $2\ \mu m$, and at the output end of the fiber, Fresnel reflection was used for feedback and output coupling. To avoid introducing aberrations to the $2\ \mu m$ output, a 2 mm thick

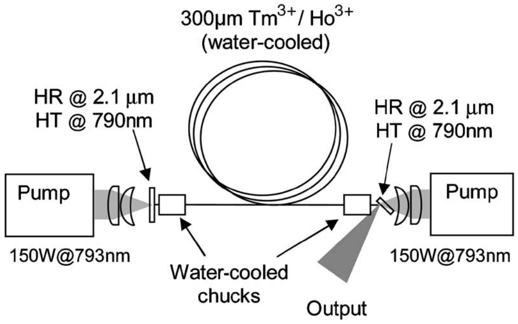

Fig. 1. Schematic diagram of the experimental setup. HR, highly reflecting; HT, highly transmitting.

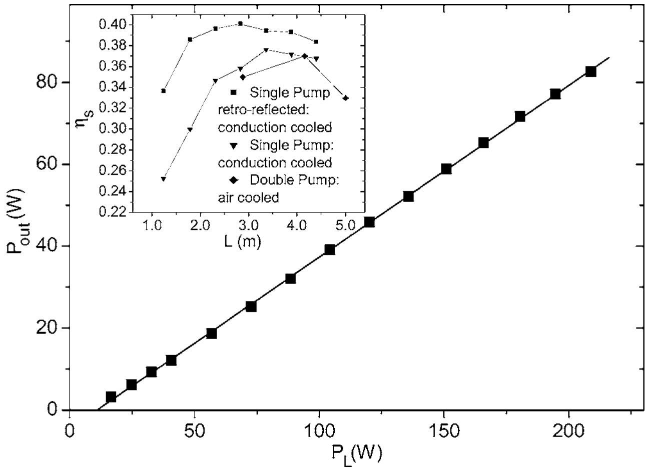

Fig. 2. Output power, P_{out}, from the $L=4.2$ m fiber laser measured as function of the launched pump power, P_L. The inset displays the slope efficiency, η_S, of the fiber laser output measured as a function of the length, L, of the double-clad fiber when the fiber was pumped from either one end or both ends.

highly reflective 2.1 μm dichroic output mirror was oriented ~20° relative to the axis of the fiber, causing a slight reduction in the launch efficiency. The fiber ends were cooled by using water-cooled chucks with the excess heat removed from the remaining coiled fiber by either (1) forced-air cooling provided by a fan mounted above, (2) conduction cooling where the fiber is wrapped tightly onto a cooled aluminum spool, or (3) immersion in a water bath. For pumping the laser, two water-cooled 150 W, 793 nm modules containing beam-shaped diode laser bars were available, which were directly coupled into the active fiber. The launch efficiency of ~72% into the 300 μm diameter pump core of the fiber was determined by using the cutback method.

In the first set of experiments, only one end of the fiber was pumped (in an arrangement similar to Fig. 1), and the output power was measured with and without a pump retroreflecting mirror at the output end to the fiber. The inset to Fig. 2 shows the typical slope efficiency variation with the change in the fiber length. As expected, pump retroreflection at the output end allows for a wider choice of fiber length as compared with Fresnel reflection only, a characteristic that can also be expected for double-end pumping. A limited data set was recorded for the performance of the fiber laser pumped from both ends, under conditions of forced-air cooling, indicating that the optimum length for this mode of operation was ~4 m.

The output power from a 4.2 m length fiber laser as a function of the launched pump power into both ends of the fiber is shown in Fig. 2 (note that water-cooled operation was employed). The maximum output power of 83 W from the fiber laser was measured, and the maximum slope efficiency for the 4.2 m fiber length was 42% as a function of the launched pump power, P_L. Considering that the Stokes efficiency limit is 38%, this result suggests that some cross relaxation among the Tm^{3+} ions is aiding the overall excitation of the Ho^{3+} ions. The maximum output power from the fiber laser was limited by the thermally induced damage, which manifest as a catastrophic melting of the fiber ends.

The beam quality of the output from the dual-end-pumped arrangement was carefully measured by using two CaF_2 wedges in series to reduce the average power followed by an $f=500$ mm AR-coated plano–convex ZnSe singlet lens. The results of the beam waist measurements (obtained by fitting a Gaussian line shape to images recorded on a Spiricon Pyrocam III) as a function of distance each side of the focus is shown in Fig. 3. The values of the beam quality parameter in each transverse dimension were calculated to be $M^2=1.3$ for the laser power of 2 W, rising slightly to $M^2=1.5$ for the laser power of 65 W. A possible reason for the lower-than diffraction-limited beam quality is the use of nondiffraction-limited plano–convex lenses. At higher power the thermally induced refractive index profile may further degrade the beam quality.

Figure 4 displays the optical spectrum of the output from the fiber laser for two values of the output power. For low-output (pump) power, the output spectrum displays emission with a central wavelength of 2100 nm and a bandwidth of approximately 6 nm. This emission relates to the Ho^{3+} ion only, since the fiber length is too short for very long wavelength emission from the Tm^{3+} ion. As the output (pump) power is increased to 65 W, both the central wavelength and bandwidth of the emission increase to 2106 nm and >10 nm, respectively. The 65 W output was produced for $P_L=189$ W; thus the heat load within the fiber can be estimated to be approximately 31 Wm^{-1}. Boltzmann filling of the Stark levels of the $^5I_8$ ground state from the heat forces emission to higher Stark levels.

Figure 5 displays the measured output power from the dual-end-pumped 4.2 m long fiber laser over a time period of 39 s at a power level of 55 W using a 200 MHz bandwidth dc-coupled detector and a sampling interval of 4 ms. The calculated standard devia-

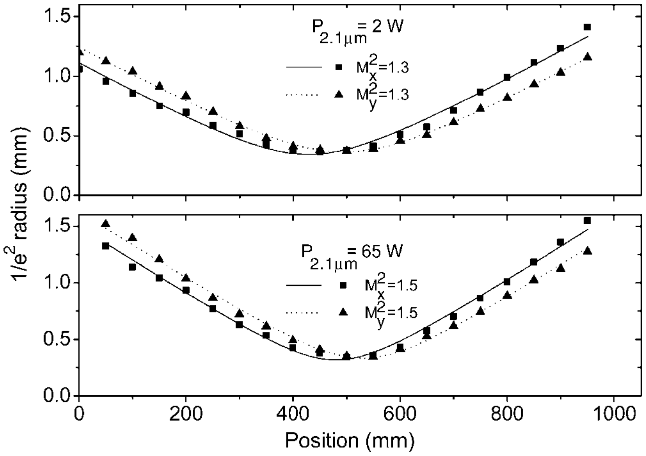

Fig. 3. Measurements of the beam radius as a function of the distance from the focus of an $f=500$ mm AR-coated plano–convex ZnSe singlet lens. The beam quality was measured when the output power from the fiber laser was 2 and 65 W. $L=4.2$ m.

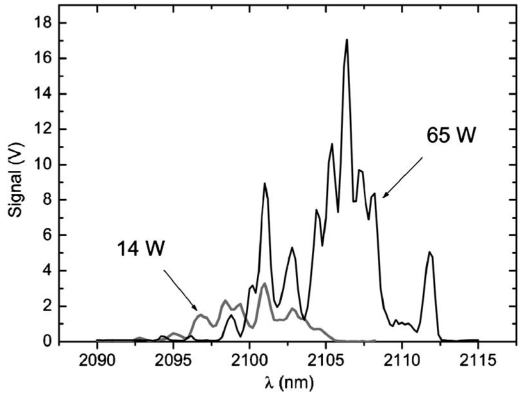

Fig. 4. Measured spectrum of the fiber laser output for two values of the output power. $L=4.2$ m. Note spectrum was recorded over 1800–2150 nm with no laser emission observed for wavelengths <2092 nm.

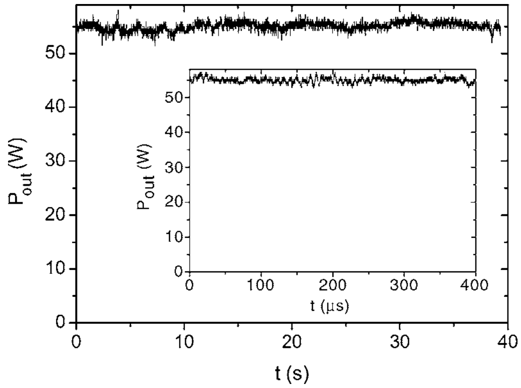

Fig. 5. Measurements of the output from the $L=4.2$ m fiber laser taken over a 39 s period. The inset displays the variation in the fiber laser output over a 400 μs time period.

tion of 1.1 W corresponds to a stability of ±2%. The inset to Fig. 5 shows the amplitude stability recorded over a reduced time period of 400 μs and shows the dominant source of noise to be oscillations of ~ 10 μs period—oscillations that are likely related to the relaxation oscillation frequency of the fiber laser. The dual-end-pumping scheme provides a near-uniform population inversion along the fiber length, and hence oscillations relating to saturable absorption of the laser emission are minimized.

The maximum slope efficiency generated from the current fiber laser is slightly greater than the Stokes efficiency limit and is similar to the slope efficiencies presented in recent reports.[11,12] Some scope for improvement in the efficiency may be provided from an increase in the Tm^{3+} to Ho^{3+} concentration ratio; however, some improvement may also be gained from a change in the value of the output coupling.

On the basis of slope efficiency considerations alone, alternative fiber laser configurations, which rely on tandem pumping with the output from either an Yb^{3+}-doped silica fiber laser[13] or a Tm^{3+}-doped silica fiber laser[14] can outperform the present laser. For example, for the Yb^{3+}-doped and the Tm^{3+}-doped silica fiber laser-pumped systems, the Stokes efficiency limit product is 0.46 and 0.56 (if we assume that the quantum efficiency of the cross-relaxation process is 1.5), respectively. The present system, despite a large quantum defect of ~ 0.6, is comparatively less complex.

We have demonstrated a high-power and efficient holmium-doped silica fiber laser. The maximum output power was 83 W, and the slope efficiency was 42%. The room temperature operation, simple configuration, and high beam quality characteristics of this fiber laser ensure that the directly diode-pumped Tm^{3+}-Ho^{3+}-doped silica fiber laser can be used for a wide range of future applications.

The authors are grateful for financial assistance from the Australian Research Council. S. D. Jackson's e-mail address is s.jackson@oftc.usyd.edu.au. D. G. Lancaster's e-mail address is david.lancaster@dsto.defence.gov.au.

References

1. Y. Jeong, J. K. Sahu, D. N. Payne, and J. Nilsson, Opt. Express **12**, 6088 (2004).
2. A. Liem, J. Limpert, H. Zellmer, and A. Tunnermann, Opt. Lett. **28**, 1537 (2003).
3. F. Roser, J. Rothhard, B. Ortac, A. Liem, O. Schmidt, T. Schreiber, J. Limpert, and A. Tunnermann, Opt. Lett. **30**, 2754 (2005).
4. G. Frith, D. G. Lancaster, and S. D. Jackson, Electron. Lett. **41**, 687 (2005).
5. D. C. Hanna, R. M. Percival, R. G. Smart, J. E. Townsend, and A. C. Tropper, Electron. Lett. **25**, 593 (1989).
6. K. Oh, T. F. Morse, A. Kilian, L. Reinhart, and P. M. Weber, Opt. Lett. **19**, 278 (1994).
7. R. Beck and K. Gürs, J. Appl. Phys. **46**, 5224 (1975).
8. H. Lotem, Y. Kalisky, J. Kagan, and D. Sagie, IEEE J. Quantum Electron. **24**, 1193 (1988).
9. Y. Kalisky, J. Kagan, H. Lotem, and D. Sagie, Opt. Commun. **65**, 359 (1988).
10. P. A. Budni, C. A. Miller, M. L. Lemons, P. A. Ketteridge, L. A. Pomeranz, T. M. Pollak, P. G. Schunemann, S. D. Setzler, K. L. Lanier, J. R. Mosto, and E. P. Chicklis, in *Proceedings of IEEE Lasers and Electro-Optics Society (LEOS) 13th Annual Meeting* (IEEE, 2000), pp. 609–610.
11. S. D. Jackson, IEEE Photon. Technol. Lett. **18**, 1885 (2006).
12. S. D. Jackson and S. Mossman, Appl. Phys. B **77**, 489 (2003).
13. S. D. Jackson, Appl. Phys. B **76**, 793 (2003).
14. S. D. Jackson, IEEE J. Quantum Electron. **42**, 187 (2006).